

1           **A total energy error analysis of dynamical cores and**  
2           **physics-dynamics coupling in the Community Atmosphere**  
3           **Model (CAM)**

4           **Peter H. Lauritzen<sup>1\*</sup>, and David L. Williamson<sup>1</sup>**

5           <sup>1</sup>National Center for Atmospheric Research, Boulder, Colorado, USA

6           **Key Points:**

- 7           • Spurious total energy dissipation in dynamical core is  $-0.3W/m^2$  to  $-1W/m^2$  at 1  
8           degree  
9           • Constant-pressure assumption in physics leads to  $0.3W/m^2$  spurious total energy  
10           source  
11           • There can easily be compensating errors in total energy budget

---

\*1850 Table Mesa Drive, Boulder, Colorado, USA

Corresponding author: Peter Hjort Lauritzen, pel@ucar.edu

12 **Abstract**

13 A closed total energy (TE) budget is of utmost importance in coupled climate system  
 14 modeling; in particular, the dynamical core or physics-dynamics coupling should ideally  
 15 not lead to spurious TE sources/sinks. To assess this in a global climate model, a detailed  
 16 analysis of the spurious sources/sinks of TE in NCAR's Community Atmosphere Model  
 17 (CAM) is given. This includes spurious sources/sinks associated with the parameteriza-  
 18 tion suite, the dynamical core, TE definition discrepancies and physics-dynamics coupling.  
 19 The latter leads to a detailed discussion of the pros and cons of various physics-dynamics  
 20 coupling methods commonly used in climate/weather modeling.

21 **1 Introduction**

22 In coupled climate modeling with prognostic atmosphere, ocean, land, land-ice, and  
 23 sea-ice components, it is important to conserve total energy (TE) to a high degree in each  
 24 component individually and in the complete model to avoid spurious long term trends in  
 25 the simulated Earth system. Conservation of TE in this context refers to having a closed  
 26 TE budget. For example, the TE change in a column in the atmosphere is exactly balanced  
 27 by the net sources/sinks given by the fluxes through the column. The fluxes into the at-  
 28 mospheric component from the surface models must be balanced by the fluxes in the re-  
 29 spective surface components and so on. Henceforth we will focus only on the atmospheric  
 30 component which, in a numerical model, is split into a resolved-scale component (the dy-  
 31 namical core) and a sub-grid-scale component (parameterizations or, in modeling jargon,  
 32 physics). While there have been many studies on energy flow in the Earth system through  
 33 analysis of re-analysis data and observations [Trenberth and Fasullo, 2018, and references  
 34 herein], there has been less focus on spurious TE sources/sinks in numerical models.

35 The atmospheric equations of motion conserve TE but the discretizations used in cli-  
 36 mate and weather models are usually not inherently TE conservative. Exact conservation  
 37 is probably not necessary but conservation to within  $\sim 0.01 \text{ W/m}^2$  has been considered  
 38 sufficient to avoid spurious trends in century long simulations [Boville, 2000; Williamson  
 39 *et al.*, 2015]. Spurious sources and sinks of TE can be introduced by the dynamical core,  
 40 physics, physics-dynamics coupling as well as discrepancies between the TE of the con-  
 41 tinuous and discrete equations of motion and for the physics. Hence the study of TE con-  
 42 servation in comprehensive models of the atmosphere quickly becomes a quite complex  
 43 and detailed matter. In addition there can easily be compensating errors in the system as a  
 44 whole.

45 Here we focus on versions of the Community Atmosphere Model (CAM) that use  
 46 the spectral-element [SE, Lauritzen *et al.*, 2018] and finite-volume [FV, Lin, 2004] dy-  
 47 namical cores. These dynamical cores couple with physics in a time-split manner, i.e.  
 48 physics receives a state updated by dynamics [see Williamson, 2002, for a discussion  
 49 of time-split versus process split physics-dynamics coupling in the context of CAM]. In  
 50 its pure time-split form the physics tendencies are added to the state previously produced  
 51 by the dynamical core and the resulting state provides the initial state for the subsequent  
 52 dynamical core calculation. We refer to this as *state-updating* (`ftype=1` in CAM code).  
 53 Alternatively, when the dynamical core adopts a shorter time step than the physics, say  
 54 `nsplit` sub-steps, then  $(1/\text{nsplit})$ th of the physics-calculated tendency is added to the  
 55 state before each dynamics sub-step. We refer to this modification of time-splitting as  
 56 *dribbling* (`ftype=0`). CAM-FV uses the *state-update* (`ftype=1`) approach while CAM-SE  
 57 has options to use *state-update* (`ftype=1`), *dribbling* (`ftype=0`) or a combination of the  
 58 two i.e. mass-variables use *state-updating* and remaining variables use *dribbling*. We refer  
 59 to this as *combination* (`ftype=2`). The *dribbling* variants can lead to spurious sources or  
 60 sinks of TE (and mass) referred to here as physics-dynamics coupling errors.

61 The dynamical core usually has inherent or specified filters to control spurious noise  
 62 near the grid scale which will lead to energy dissipation [Thuburn, 2008; Jablonowski

and Williamson, 2011]. Similarly models often have sponge layers to control the solution near the top of the model that may be a sink of TE. There are examples of numerical discretizations of the adiabatic frictionless equations motion that are designed so that TE is conserved in the absence of time-truncation and filtering errors [e.g., Eldred and Randall, 2017; McRae and Cotter, 2013], e.g., mimetic spectral-element discretizations such as the one used in the horizontal in CAM-SE [Taylor, 2011]. These provide consistency between the discrete momentum and thermodynamic equations leading to global conservation associated with the conversion of potential to kinetic energy. In spectral transform models it is customary to add the energy change due to explicit diffusion on momentum back as heating (referred to as frictional heating), so that the diffusion of momentum does not affect the TE budget [see, e.g., p.71 in Neale et al., 2012]. This is also done in CAM-SE [Lauritzen et al., 2018].

The purpose of this paper is to provide a detailed global TE analysis of CAM. We assess TE errors due to various steps in the model algorithms. The paper is outlined as follows. In section 2 the continuous TE formulas are given and a detailed description of spurious TE sources/sinks that can occur in a model as a whole, and the associated diagnostics used to perform the TE analysis, are defined. In section 3 the model is run in various configurations to assess their effects on TE conservation. This includes various physics-dynamics coupling experiments leading to a rather detailed discussion of mass budget closure. We also investigate the effect of using a limiter in the vertical remapping of momentum, assess energy discrepancy errors and impacts on TE of simplifying surface conditions and dry atmosphere experiments. The paper ends with conclusions.

## 2 Method

### 2.1 Defining total energy (TE)

In the following it is assumed that the model top and bottom are coordinate surfaces and that there is no flux of mass through the model top and bottom. In a dry hydrostatic atmosphere the TE equation integrated over the entire sphere is given by

$$\frac{d}{dt} \int_{z=z_s}^{z=z_{top}} \iint_S E_v \rho^{(d)} dA dz = \int_{z=z_s}^{z=z_{top}} \iint_S F_{net} \rho^{(d)} dA dz, \quad (1)$$

[e.g., Kasahara, 1974] where  $F_{net}$  is net flux calculated by the parameterizations (e.g., heating and momentum forcing),  $d/dt$  the total/material derivative,  $z_s$  is the height of the surface,  $S$  the sphere,  $\rho^{(d)}$  the density of dry air,  $E_v$  is the TE and  $dA$  is an infinitesimal area on the sphere.  $E_v$  can be split into kinetic energy  $K = \frac{1}{2}\mathbf{v}^2$  ( $\mathbf{v}$  is the wind vector), internal energy  $c_v^{(d)}T$ , where  $c_v^{(d)}$  is the heat capacity of dry air at constant volume, and potential energy  $\Phi = gz$

$$E_v = K + c_v^{(d)}T + \Phi. \quad (2)$$

If the vertical integral is performed in a mass-based vertical coordinate, e.g., pressure, then the integrated TE equation for a dry atmosphere can be written as

$$\frac{d}{dt} \int_{p=p_s}^{p=p_{top}} \iint_S E_p \rho^{(d)} dA dp + \frac{d}{dt} \iint_S \Phi_s p_s dA = \int_{p=p_s}^{p=p_{top}} \iint_S F_{net} \rho dA dp, \quad (3)$$

[e.g., Kasahara, 1974] where

$$E_p = K + c_p^{(d)}T. \quad (4)$$

In a moist atmosphere, however, there are several definitions of TE used in the literature related to what heat capacity is used for water vapor and whether or not condensates are accounted for in the energy equation. To explain the details of that we focus on the energy equation for CAM-SE.

CAM-SE is formulated using a terrain-following hybrid-sigma vertical coordinate  $\eta$  but the coordinate levels are defined in terms of dry air mass per unit area ( $M^{(d)}$ ) instead of total air mass;  $\eta^{(d)}$  [see Lauritzen et al., 2018, for details]. In such a coordinate

106 system it is convenient to define the tracer state in terms of a dry mixing ratio instead of  
 107 moist mixing ratio

$$m^{(\ell)} \equiv \frac{\rho^{(\ell)}}{\rho^{(d)}}, \text{ where } \ell = 'wv', 'cl', 'ci', 'rn', 'sw', \quad (5)$$

108 where  $\rho^{(d)}$  is the mass of dry air per unit volume of moist air and  $\rho^{(\ell)}$  is the mass of the  
 109 water substance of type  $\ell$  per unit volume of moist air. Moist air refers to air containing  
 110 dry air ('d'), water vapor ('wv'), cloud liquid ('cl'), cloud ice ('ci'), rain amount ('rn')  
 111 and snow amount ('sw'). For notational purposes define the set of all components of air

$$\mathcal{L}_{all} = \{'d', 'wv', 'cl', 'ci', 'rn', 'sw'\}, \quad (6)$$

112 Define associated heat capacities at constant pressure  $c_p^{(\ell)}$ . We refer to condensates as being  
 113 *thermodynamically active* if they are included in the thermodynamic equation and mo-  
 114 mentum equations. E.g. if the thermodynamic equation is formulated in terms of temper-  
 115 ature the energy conversion term includes a generalized heat capacity which is a function  
 116 of the condensates and their associated heat capacities [see, e.g., section 2.3 in *Lauritzen*  
 117 *et al.*, 2018]. Similarly the weight of the condensates is included in the pressure field and  
 118 pressure gradient force. How many and which condensates are thermodynamically ac-  
 119 tive in the dynamical core is controlled with namelist `qsize_condensate_loading`. If  
 120 `qsize_condensate_loading=1` only water vapor ('wv') is active, `qsize_condensate_loading=3`  
 121 'wv', 'cl', and 'ci' are active, and if `qsize_condensate_loading=5` then 'wv', 'cl', 'ci', 'rn',  
 122 and 'sw' are included.

123 Using the  $\eta^{(d)}$  vertical coordinate and dry mixing ratios the TE (per unit area) that  
 124 the frictionless adiabatic equations of motion in the CAM-SE dynamical core conserves is

$$\widehat{E}_{dyn} = \frac{1}{\Delta S} \int_{\eta=0}^{\eta=1} \iint_S \left( \frac{1}{g} \frac{\partial M^{(d)}}{\partial \eta^{(d)}} \right) \sum_{\ell \in \mathcal{L}_{all}} \left[ m^{(\ell)} (K + c_p^{(\ell)} T + \Phi_s) \right] dA d\eta^{(d)}, \quad (7)$$

125 where  $\Delta S$  is the surface area of the sphere,  $\Phi_s$  is the surface geopotential and  $(\cdot)$  refers to  
 126 the global average.

127 In the CAM physical parameterizations a different definition of TE is used. Due to  
 128 the evolutionary nature of the model development, the parameterizations have not yet been  
 129 converted to match the SE dynamical core. For the computation of TE, condensates are  
 130 assumed to be zero and the heat capacity of moisture is the same as for dry air. This is  
 131 equivalent to using a moist mass (dry air plus water vapor) but  $c_p$  of dry air:

$$\widehat{E}_{phys} = \frac{1}{\Delta S} \int_{\eta=0}^{\eta=1} \iint_S \left( \frac{1}{g} \frac{\partial M^{(d)}}{\partial \eta^{(d)}} \right) (1 + m^{(wv)}) \left[ (K + c_p^{(d)} T + \Phi_s) \right] dA d\eta^{(d)}. \quad (8)$$

132 We note that earlier versions of CAM using the spectral transform dynamical core used  
 133  $c_p$  of moist air. The adiabatic, frictionless equations of motion in the CAM-SE dynamical  
 134 core can be made consistent with  $E_{phys}$  by not including condensates in the mass/pressure  
 135 field as well as energy conversion term in the thermodynamic equation and setting the  
 136 heat capacity for moisture to  $c_p^{(d)}$  [Taylor, 2011]. We refer to this version of CAM-SE as  
 137 the *energy consistent* version.

## 138 2.2 Spurious energy sources and sinks

139 In a weather/climate model TE conservation errors can appear in many places through-  
 140 out the algorithm. Below is a general list of where conservation errors can appear with  
 141 specific examples from CAM:

- 142 1. *Parameterization errors*: Individual parameterizations may not have a closed en-  
 143 ergy budget. CAM parameterizations are required to have a closed energy budget  
 144 under the assumption that pressure remains constant during the computation of the

145 subgrid-scale parameterization tendencies. In other words, the TE change in the  
 146 column is exactly balanced by the net sources/sinks given by the fluxes through the  
 147 column.

- 148 2. *Pressure work error*: That said, if parameterizations update specific humidity then  
 149 the surface pressure changes (e.g., moisture entering or leaving the column). In  
 150 that case the pressure changes which, in turn, changes TE. This is referred to as  
 151 *pressure work error* [section 3.1.8 in *Neale et al.*, 2012].
- 152 3. *Continuous TE formula discrepancy*: If the continuous equations of motion for the  
 153 dynamical core conserve a TE different from the one used in the parameterizations  
 154 then an energy inconsistency is present in the system as a whole. This is the case  
 155 with the new version of CAM-SE that conserves a TE that is more accurate and  
 156 comprehensive than that used in the CAM physics package as discussed above. As  
 157 also noted above, this mismatch arose from the evolutionary nature of the model  
 158 development and not by deliberate design; and should be eliminated in the future.
- 159 4. *Dynamical core errors*: [mention that we assume that dynamical core is inherently  
 160 **mass conservative**] Energy conservation errors in the dynamical core, not related to  
 161 physics-dynamics coupling errors, can arise in multiple parts of the algorithms used  
 162 to solve the equations of motion. For dynamical cores employing filtering [e.g.,  
 163 limiters in flux operators *Lin*, 2004] and/or possessing inherent damping which  
 164 controls small scales, it is hard to isolate their energy dissipation from other errors  
 165 in the discretization. If a hyperviscosity term or some other diffusion is added to  
 166 the momentum equation, then one can diagnose the local energy dissipation from  
 167 such damping and add a corresponding heating to balance it (frictional heating).  
 168 There may also be energy loss from viscosity applied to other variables such a tem-  
 169 perature or pressure which is harder to compensate. Here is a break-down relevant  
 170 to CAM-SE using a floating Lagrangian vertical coordinate:
  - 171 • Horizontal inviscid dynamics: Energy errors resulting from solving the inviscid,  
 172 adiabatic equations of motion.
  - 173 • Hyperviscosity: Filtering errors.
  - 174 • Vertical remapping: The vertical remapping algorithm from Lagrangian to Eule-  
 175 rian reference surfaces does not conserve TE.
  - 176 • Near round-off negative values of water vapor which are filled to a minimal  
 177 value without compensation.
- 178 5. *Physics-dynamics coupling (PDC)*: Assume that physics computes a tendency. Usu-  
 179 ally the tendency (forcing) is passed to the dynamical core which is responsible for  
 180 adding the tendencies to the state. PDC energy errors can be split into three types:
  - 181 • ‘Dribbling’ errors (or, equivalently, temporal PDC errors): If the TE increment  
 182 from the parameterizations does not match the change in TE when the tenden-  
 183 cies are added to the state in the dynamical core, then there will be a spurious  
 184 PDC error. This will not happen with the *state-update* approach in which the  
 185 tendencies are added immediately after physics and before the dynamical core  
 186 advances the solution in time.
  - 187 PDC errors in temperature (and velocity) tendencies occur because the *T*-increment  
 188 (call it  $\Delta T$ ) that the parameterizations prescribe leads to a dry thermal energy  
 189 change of  $\Delta M^{(d)}\Delta T$  which will not match the dry thermal energy change when  
 190 the temperature tendency is added in smaller chunks in the dynamical core dur-  
 191 ing the ‘dribbling’ of  $\Delta T$ . The reason being that  $\Delta M^{(d)}$  changes during each  
 192 time-step and hence the thermal energy change due to physics forcing accumu-  
 193 lated during the ‘dribbling’ will not equal  $\Delta M^{(d)}\Delta T$ . This error could possibly  
 194 be eliminated by using thermal energy forcing instead of temperature increments.  
 195 [mention that PDC errors can be divided into mass ‘clipping’ errors and internal  
 196 energy and kinetic energy.]
  - 197 • Change of vertical grid/coordinate errors: If the vertical coordinates in physics  
 198 and in the dynamical core are different then there can be spurious PDC energy

199 errors even when using the state-update method for adding tendencies to the dy-  
 200 namical core state. For example, many non-hydrostatic dynamical cores [e.g.  
 201 *Skamarock et al.*, 2012] use a terrain-following height coordinate whereas physics  
 202 uses pressure.

- 203 • *Change of horizontal grid errors:* If the physics tendencies are computed on a  
 204 different horizontal grid than the dynamical core then there can be spurious en-  
 205 ergy errors from mapping tendencies and/or variables between horizontal grids  
 206 [e.g., *Herrington et al.*, 2018].

207 6. *Compensating Energy fixers:* To avoid TE conservation errors which could accu-  
 208 mulate and ultimately lead to a climate drift, it is customary to apply an arbitrary  
 209 energy fixer to restore TE conservation. Since the spatial distribution of many en-  
 210 ergy errors, in general, is not known, global fixers are used. In CAM a uniform in-  
 211 crement is added to the temperature field to compensate for TE imbalance from all  
 212 processes, i.e. dynamical core, physics-dynamics coupling, TE formula discrepancy,  
 213 energy change due to pressure work **error**, and possibly parameterization errors if  
 214 present.

### 215 2.3 Diagnostics

216 The discrete global averages  $\widehat{(\cdot)}$  are computed consistent with the discrete model grid  
 217 as outlined in section 2.2. of *Lauritzen et al.* [2014]. The TE global average tendency is  
 218 denoted

$$\partial \widehat{E} \equiv \frac{d\widehat{E}}{dt}. \quad (9)$$

219 By computing the global TE averages  $\widehat{E}$  at appropriate places in the model algorithms,  
 220 we can directly compute  $\partial \widehat{E}$  due to various processes (such as viscosity, vertical remap-  
 221 ping, physics-dynamics coupling, pressure work **error**, etc.) by differencing  $\widehat{E}$  from after  
 222 and before the algorithm takes place. This has been implemented using CAM history in-  
 223 frastructure by computing column integrals of energy at various places in CAM and out-  
 224 putting the 2D energy fields. CAM history internally handles accumulation and averag-  
 225 ing in time at each horizontal grid point. The global averages are computed externally  
 226 from the grid point vertical integrals on the history files (stored in double precision). The  
 227 places in CAM where we compute/capture the grid point vertical integral  $E$  are named us-  
 228 ing three letters where the first letter refers to whether the vertical integral is performed  
 229 in physics ('p') or in the dynamical core ('d'). The trailing two letters refer to the specific  
 230 location in dynamics or physics. For example, 'BP' refers to 'Before Physics' and 'AP'  
 231 to 'After Physics'; the associated total energies are denoted  $E_{pBP}$  and  $E_{pAP}$ , respectively.  
 232 The TE tendency from the parameterizations is the difference between  $E_{pBP}$  and  $E_{pAP}$   
 233 divided by the time-step. The terms and tendencies are then averaged globally externally  
 234 to the model. The pseudo-code in Figure 1 defines the acronyms in terms of where in the  
 235 CAM-SE algorithm the TE vertical integrals are computed and output. For details on the  
 236 CAM-SE algorithm please see *Lauritzen et al.* [2018].

237 Before defining the individual terms in detail we briefly review the model time step-  
 238 ping sequence starting with the physics component as illustrated in Figure 1. The energy  
 239 fixer is applied first to compensate for the spurious net energy change from all compo-  
 240 nents introduced during the previous time step. We will describe this in more detail af-  
 241 ter the various sources and sinks are elucidated. The parameterizations are applied next  
 242 and are required to be energy conserving. They update the state and accumulate the total  
 243 physics tendency (forcing). At this stage the state is saved for use in the energy fixer in  
 244 the next time step. Any changes in the global average energy after this are spurious and  
 245 are compensated by the fixer. The parameterizations update the water vapor but not the  
 246 moist pressure, implying a non-physical change in the dry mass of the atmosphere. The  
 247 dry mass correction corrects the dry mass back to its proper value.

The forcing (physics tendency) from the parameterizations is passed to the dynamical core. If the physics and dynamics operate on different grids, the forcing is remapped here. The dynamics operates on a shorter time step than the physics and is sub-stepped. The remapped forcing is applied to the dynamics state, saved from the end of the previous dynamics step, using either *state-updating*, *dribbling*, or *combination* as described in the introduction. The dynamics then advances the adiabatic frictionless flow in the floating Lagrangian layers over a further set of sub-steps. Hyperviscosity is applied next with further sub-stepping required for computational stability of the explicit discrete approximations. The energy loss from the specified momentum viscosity is calculated locally and is balanced by adding a local change to the temperature, referred to as *frictional heating*. This set of dynamics sub-steps is followed by the vertical remapping from Lagrangian to Eulerian reference layers. The remapping is required to provide layers consistent with the parameterization formulations. The vertical remapping sub-steps are required for stability if the Lagrangian layers become too thin.

At the end of the dynamics, the state is saved to be used by the dynamics the next time step and is also passed to the physics, with a remapping if the dynamics and physics grids differ. At the beginning of the physics the difference in energy between this state and the state saved after the physics during the previous time step is the amount needed to be added or subtracted by the energy fixer. It represents the accumulation of all spurious sources from the dry mass correction, remappings between physics and dynamics grids (if applicable), dynamical core, differing energy definitions (if present), hyperviscosity, and vertical remapping.

We now define the following energy tendencies corresponding to the itemized list in section 2.2 with references to terms indicated in Figure 1. We start just after the energy fixer which will be defined at the end.

1.  $\partial\widehat{E}^{(param)}$ : TE tendency due to parameterizations. In CAM the TE budget for each parameterization is closed (assuming pressure is unchanged) so  $\partial\widehat{E}^{(param)}$  is balanced by net fluxes in/out of the physics columns. Note that this is the only energy tendency that is not spurious since CAM parameterizations have a closed TE budget. This TE tendency is discretely computed as

$$\partial\widehat{E}_{phys}^{(param)} = \frac{\widehat{E}_{pAP} - \widehat{E}_{pBP}}{\Delta t_{phys}}, \quad (10)$$

where  $\Delta t_{phys}$  is the physics time-step (default 1800s) and the subscript *phys* on  $\partial\widehat{E}$  refers to the energy tendency computed in CAM physics.

2.  $\partial\widehat{E}^{(pwork)}$ : Total spurious energy tendency due to pressure work **error**

$$\partial\widehat{E}_{phys}^{(pwork)} = \frac{\widehat{E}_{pAM} - \widehat{E}_{pAP}}{\Delta t_{phys}}. \quad (11)$$

Since CAM-SE dynamical core is based on a dry-mass vertical coordinate the pressure work **error** takes place implicitly in the dynamical core. But the TE tendency due to pressure work **error** is conveniently computed in physics since dynamical cores based on a moist vertical coordinate (e.g., CAM-FV) require pressure and moist mixing ratios to be adjusted for dry mass conservation and tracer mass conservation [section 3.1.8 in *Neale et al.*, 2012]. The difference of TE after and before this adjustment is the TE tendency due to pressure work **error**. In a dry mass vertical coordinate based on dry mixing ratios neither dry mass layer thickness nor dry mixing ratios need to be adjusted to take into account moisture changes in the column. For labeling purposes, the 'total forcing' associated with physics (at least in CAM) consists of parameterizations, pressure work **error** and TE fixer, although strictly speaking the fixer includes components from the dynamics as will be seen.

$$\partial\widehat{E}_{phys}^{(phys)} \equiv \partial\widehat{E}_{phys}^{(param)} + \partial\widehat{E}_{phys}^{(pwork)} + \partial\widehat{E}_{phys}^{(efix)} = \frac{\widehat{E}_{pAM} - \widehat{E}_{pBF}}{\Delta t_{phys}}. \quad (12)$$

301 where the energy fixer TE tendency is

$$\partial \widehat{E}_{phys}^{(efix)} = \frac{\widehat{E}_{pBP} - \widehat{E}_{pBF}}{\Delta t_{phys}}. \quad (13)$$

302 After all the TE budget terms have been defined, the exact composition of  $\partial \widehat{E}_{phys}^{(efix)}$   
303 will be presented.

- 304 3.  $\partial \widehat{E}^{(discr)}$ : If the physics uses a TE definition different from the TE that the  
305 continuous equations of motion in the dynamical core conserve (i.e. in the absence of  
306 discretization errors), then there is a TE discrepancy tendency. This complicates  
307 the energy analysis as one can not compare TE computed in physics  $\widehat{E}_{phys}$  directly  
308 with TE computed in the dynamical core  $\widehat{E}_{dyn}$ . This makes errors associated with  
309 this discrepancy tricky to assess. That said, the TE tendencies computed using the  
310 dynamical core TE formula  $\partial \widehat{E}_{dyn}$  are well defined (self consistent) and similarly  
311 for TE tendencies computed using the ‘physics formula’ for TE,  $\partial \widehat{E}_{phys}$ .
- 312 4. The TE tendency from the dynamical core is split into several terms: Horizontal  
313 adiabatic dynamics (dynamics excluding physics forcing tendency)

$$\partial \widehat{E}_{dyn}^{(2D)} = \frac{\widehat{E}_{dAD} - \widehat{E}_{dBd}}{\Delta t_{dyn}}, \quad (14)$$

314 where over a single dynamics sub-step  $\Delta t_{dyn} = \frac{\Delta t_{phys}}{\text{nsplit} \times \text{rsplit}}$  (the loop bounds  
315 `nsplit`, `rsplit`, etc. are explained in Figure 1).

316 In CAM-SE the viscosity is explicit so one can compute the TE tendency due to  
317 hyperviscosity and its associated frictional heating

$$\partial \widehat{E}_{dyn}^{(hvvis)} = \frac{\widehat{E}_{dAH} - \widehat{E}_{dBH}}{\Delta t_{hvvis}}, \quad (15)$$

318 which, in CAM-SE, includes a frictional heating term from viscosity on momentum

$$\partial \widehat{E}_{dyn}^{(fheat)} = \frac{\widehat{E}_{dAH} - \widehat{E}_{dCH}}{\Delta t_{hvvis}}, \quad (16)$$

319 where  $\Delta t_{hvvis} = \frac{\Delta t_{phys}}{\text{nsplit} \times \text{rsplit} \times \text{hypervis\_subcycle}}$  is the time step of the sub-stepped  
320 viscosity. The residual

$$\partial \widehat{E}_{dyn}^{(res)} = \partial \widehat{E}_{dyn}^{(2D)} - \partial \widehat{E}_{dyn}^{(hvvis)}, \quad (17)$$

321 is the energy error due to inviscid dynamics and time-truncation errors.

322 The energy tendency due to vertical remapping is

$$\partial \widehat{E}_{dyn}^{(remap)} = \frac{\widehat{E}_{dAR} - \widehat{E}_{dAD}}{\Delta t_{remap}}, \quad (18)$$

323 where  $\Delta t_{remap} = \frac{\Delta t_{phys}}{\text{nsplit}}$ .

324 The 3D adiabatic dynamical core (no physics forcing but including friction) energy  
325 tendency is denoted

$$\partial \widehat{E}_{dyn}^{(adiab)} = \partial \widehat{E}_{dyn}^{(2D)} + \partial \widehat{E}_{dyn}^{(remap)}. \quad (19)$$

- 326 5.  $\partial \widehat{E}^{(pdc)}$ : Total spurious energy tendency due to physics-dynamics coupling errors is  
327 the difference between the energy tendency from physics and the energy tendency  
328 in the dynamics resulting from adding the physics increment to the dynamical core  
329 state

$$\partial \widehat{E}^{(pdc)} = \partial \widehat{E}_{phys}^{(phys)} - \partial \widehat{E}_{dyn}^{(phys)} \text{ assuming } \partial \widehat{E}^{(discr)} = 0, \quad (20)$$

330 where

$$\partial \widehat{E}_{dyn}^{(phys)} = \frac{\widehat{E}_{dBd} - \widehat{E}_{dAF}}{\Delta t_{pdc}}, \quad (21)$$

and  $\Delta t_{pdc}$  is the time-step between physics increments being added to the dynamical core. Remember we are dealing with average rates so terms computed with different time steps can be compared, but differences cannot be taken between terms sampled with different time steps.

The physics-dynamics coupling TE tendency  $\partial \widehat{E}^{(pdc)}$  makes use of TE formulas in dynamics and in physics so (20) is only well-defined if the TE formula discrepancy is zero,  $\partial \widehat{E}^{(discr)} = 0$ . As mentioned in Section 2.1, CAM-SE has the option to switch the continuous equations of motion conserving the TE used by CAM physics (8) instead of the more comprehensive TE formula (7).

In CAM-SE there are 3 physics-dynamics coupling algorithms described in detail in section 3.6 in *Lauritzen et al. [2018]* and reviewed in the introduction here. One is *state-update* in which the entire physics increments are added to the dynamics state at the beginning of dynamics (referred to as `ftype=1`), in which case  $\Delta t_{pdc} = \Delta t_{phys}$ . Another is *dribbling* in which the physics tendency is split into `nsplit` equal chunks and added throughout dynamics (more precisely after every vertical remapping; referred to as `ftype=0` resulting in  $\Delta t_{pdc} = \frac{1}{nspit} \Delta t_{phys}$ ), and then a *combination* of the two (referred to as `ftype=2`) where tracers (mass variables) use *state-update* (`ftype=1`) and all other physics tendencies use *dribbling* (`ftype=0`).

6.  $\partial \widehat{E}^{(efix)}$ : Global energy fixer tendency, defined in (13), is applied at the beginning of the parameterizations. The correction needed is the global average difference between the state passed from the dynamics and the state that was saved after the physics updated the state but before the dry mass correction. It includes all spurious sources from the dry mass correction, remappings between physics and dynamics, dynamical core, differing energy definitions (if present), hyperviscosity, and vertical remapping.

## 2.4 A few observations regarding the energy budget terms

It is useful to note that the energy fixer ‘fixes’ energy errors for the dynamical core, pressure work `error`, physics-dynamics coupling and TE discrepancy

$$-\partial \widehat{E}_{phys}^{(efix)} = \partial \widehat{E}_{phys}^{(pwork)} + \partial \widehat{E}_{dyn}^{(adiab)} + \partial \widehat{E}^{(pdc)} + \partial \widehat{E}^{(discr)}. \quad (22)$$

The forcing from the parameterizations,  $\partial \widehat{E}_{phys}^{(param)}$ , does not appear in this budget (although the dynamical core state does ‘feel’ the parameterization forcing) as the energy cycle for the parameterizations is, by design in CAM, closed (balanced by fluxes in/out of the physics columns). If  $\partial \widehat{E}^{(discr)} = 0$ , one can use (22) to diagnose energy dissipation in the dynamical core and physics-dynamics coupling from quantities computed only in physics

$$\partial \widehat{E}_{dyn}^{(adiab)} + \partial \widehat{E}^{(pdc)} = -\partial \widehat{E}_{phys}^{(efix)} - \partial \widehat{E}_{phys}^{(pwork)} \text{ for } \partial \widehat{E}^{(discr)} = 0. \quad (23)$$

This is useful if the diagnostics are not implemented in the dynamical core; in particular, if the *state-update* (`ftype=1`) physics-dynamics coupling method is used then  $\partial \widehat{E}^{(pdc)} = 0$  and the TE errors in the dynamical core can be computed without diagnostics implemented in the dynamical core. Also, (23) provides an alternative formula for  $\partial \widehat{E}^{(pdc)}$  compared to (20):

$$\partial \widehat{E}^{(pdc)} = -\partial \widehat{E}_{phys}^{(efix)} - \partial \widehat{E}_{phys}^{(pwork)} - \partial \widehat{E}_{dyn}^{(adiab)} \text{ assuming } \partial \widehat{E}^{(discr)} = 0. \quad (24)$$

If  $\partial \widehat{E}^{(pdc)} = 0$  (22) can be used to compute  $\partial \widehat{E}^{(discr)}$

$$\partial \widehat{E}^{(discr)} = -\partial \widehat{E}_{phys}^{(efix)} - \partial \widehat{E}_{phys}^{(pwork)} - \partial \widehat{E}_{dyn}^{(adiab)}, \text{ assuming } \partial \widehat{E}^{(pdc)} = 0. \quad (25)$$

Note that we can not use (20) to compute  $\partial \widehat{E}^{(discr)}$  since  $\widehat{E}_{phys} \neq \widehat{E}_{dyn}$ .

**Table 1.** TE tendencies in units of  $W/m^2$  associated with various aspects of CAM-SE run in AMIP-type setup (unless otherwise noted). Column 1 is the identifier for the model configuration. See the text for a brief summary of these descriptors. They are defined in more detail in the following sections where the section titles also include the ‘Descriptor’ from Table 1 to make it easier for the reader to match Table entries with discussion in the text. Column 2 is  $\mathcal{N}$  =qsize\_condensate\_loading identifying how many water species are thermodynamically active in the dynamical core (see section 2.1 for details). Column 3, lcp\_moist, indicates whether or not the heat capacity includes water variables or not and column 4 shows physics-dynamics coupling method ftype. The TE tendencies  $\partial \widehat{E}$  in columns 5-14 are defined in section 2.3. If  $\partial \widehat{E}$  is less than  $10^{-5} W/m^2$  it is set to zero in the Table. Significant changes compared to the baseline (TE consistent configuration) discussed in the main text are in bold font.

Descriptor	$\mathcal{N}$	lcp_moist	ftype	$\partial \widehat{E}_{phys}^{(pwork)}$	$\partial \widehat{E}_{phys}^{(efix)}$	$\partial \widehat{E}_{phys}^{(discr)}$	$\partial \widehat{E}_{dyn}^{(2D)}$	$\partial \widehat{E}_{dyn}^{(heat)}$	$\partial \widehat{E}_{dyn}^{(vis)}$	$\partial \widehat{E}_{dyn}^{(res)}$	$\partial \widehat{E}_{dyn}^{(fheat)}$	$\partial \widehat{E}_{dyn}^{(remap)}$	$\partial \widehat{E}_{dyn}^{(adiab)}$	$\partial \widehat{E}_{dyn}^{(pdc)}$
<i>TE consistent</i>	1	false	1	0.312	0.300	0	-0.601	-0.608	0.565	0.007	-0.011	-0.613	0	
‘dribbling’ A	1	false	0	0.315	0.313	0	-0.577	-0.584	0.568	0.007	-0.011	-0.588	<b>0.469</b>	
‘dribbling’ B	1	false	2	0.316	0.341	0	-0.598	-0.606	0.563	0.008	-0.011	-0.609	<b>0.484</b>	
<i>vert limiter</i>	1	false	1	0.317	0.472	0	-0.590	-0.597	0.509	0.006	<b>-0.199</b>	-0.789	0	
<i>smooth topo</i>	1	false	1	0.315	<b>-0.008</b>	0	<b>-0.295</b>	<b>-0.300</b>	0.493	0.005	-0.012	<b>-0.307</b>	0	
<i>energy discr</i>	5	true	1	0.332	-0.313	<b>0.594</b>	-0.603	-0.612	0.575	0.009	-0.011	-0.614	-	
<i>default</i>	5	true	2	0.316	-0.272	-0.578	-0.587	-0.579	0.579	0.010	-0.012	-0.589	-	
<i>QPC6</i>	1	false	1	0.305	-0.169	0	<b>-0.129</b>	<b>-0.131</b>	0.477	0.001	-0.007	<b>-0.136</b>	0	
<i>FHS94</i>	1	false	2	-	-	<b>-0.025</b>	<b>-0.025</b>	0.122	0	0.005	<b>-0.020</b>	-		
<i>FV</i>	1	false	1	0.304	0.670	0	-	-	-	-	<b>-0.974</b>	0		
<i>CSLAM</i>	1	false	1	0.312	0.239	0	-0.547	-0.557	0.620	0.010	-0.011	-0.558	<b>-0.070</b>	
<i>CSLAM default</i>	5	true	2	0.320	-0.342	-	-0.524	-0.537	0.641	0.013	-0.011	-0.535	-	

372 **3 Results**

373 A series of simulations have been performed with CESM2.1 using CAM version 6  
 374 (CAM6) physics (<https://doi.org/10.5065/D67H1H0V>) on NCAR's Cheyenne cluster  
 375 [*Computational and Information Systems Laboratory*, 2017]. All simulations are at nom-  
 376 inally  $\sim 1^\circ$  horizontal resolution (for CAM-SE that is  $30 \times 30$  elements on each cubed-  
 377 sphere face and for CAM-FV its  $192 \times 288$  latitudes-longitudes) and using the standard  
 378 32 levels in the vertical. Unless otherwise noted all simulations are 13 months in dura-  
 379 tion and the last 12 months are used in the analysis. Total energy budgets are summarized  
 380 in Table 1 and discussed below. The first column gives identifying 'Descriptors' which  
 381 are briefly summarized below and defined in more detail in the following sections. The  
 382 section titles also include the 'Descriptor' from Table 1 to make it easier for the reader  
 383 to match Table entries with discussion in the text. Important changes to TE errors are  
 384 marked with bold font in Table 1.

385 Various configurations are used and referred to in terms of the *COMPSET* (Com-  
 386 ponent Set) value used in CESM2.1. The *COMPSET F2000climo* configuration refers  
 387 to 'real-world' AMIP (Atmospheric Model Intercomparison Project) type simulations us-  
 388 ing perpetual year 2000 SST (Sea Surface Temperature) boundary conditions. The first 7  
 389 simulations in the table (those above the horizontal line) are such AMIP-type simulations  
 390 (*F2000climo*) with the first serving as a control for the 6 following variants. The remain-  
 391 ing 5 simulation descriptors (below the horizontal line in Table 1) list their *COMPSET* or  
 392 dynamical core settings.

- 393 • *TE consistent*: The TE consistent version uses *state update* physics-dynamics cou-  
 394 pling (*ftype* 1) described in section 3.1,
- 395 • '*dribbling*' A: as *TE consistent* but with *dribbling* physics-dynamics coupling (*ftype*  
 396  $\emptyset$ ) (section 3.2),
- 397 • '*dribbling*' B: as *TE consistent* but with *dribbling* combination physics-dynamics  
 398 coupling (*ftype* 2) (section 3.2),
- 399 • *vert limiter*: as *TE consistent* but using limiters in the vertical remapping of mo-  
 400 mentum (section 3.3),
- 401 • *smooth topo*: as *TE consistent* but using smoother topography (see section 3.4),
- 402 • *energy discr*: The version with energy discrepancy (but no physics-dynamics cou-  
 403 pling errors) described in section 3.5,
- 404 • *default*: as *energy discr* version but with *ftype=2* which is the current default  
 405 CAM-SE (section 3.5),
- 406 • *QPC6*: A simplified aqua-planet setup based on the *TE consistent*, i.e an aqua-  
 407 planet setup using CAM6 physics; an ocean covered planet in perpetual equinox,  
 408 with fixed, zonally symmetric sea surface temperatures [Neale and Hoskins, 2000;  
 409 Medeiros et al., 2016] (section 3.6),
- 410 • *FSH94*: Dry dynamical core configuration based on Held-Suarez forcing which re-  
 411 laxes temperature to a zonally symmetric equilibrium temperature profile and sim-  
 412 ple linear drag at the lower boundary [Held and Suarez, 1994] (section 3.7).,
- 413 • *FV*: A configuration with the SE dynamical core replaced with the finite-volume  
 414 core (section 3.8), and
- 415 • *CSLAM*: The quasi equal-area physics grid configuration of CAM-SE based on the  
 416 TE consistent setup (section 3.9)
- 417 • *CSLAM default*: Same as *CSLAM* configuration but with *ftype=2* and all forms of  
 418 water thermodynamically active in the dynamical core.

425           **3.1 TE consistent: state-update physics-dynamics coupling (`ftype=1`) and no TE  
426           formula discrepancy**

427     This configuration is the most energetically consistent in that the physical param-  
428     terizations and the continuous equations of motion on which the dynamical core is based,  
429     conserve the same TE (defined in equation (8)); and there are no spurious sources/sinks in  
430     physics-dynamics coupling. Energetic consistency in dynamics and physics is obtained  
431     by setting  $c_p^{(\ell)} \equiv c_p^d$  and  $\mathcal{L}_{all} = \{‘d’, ‘wv’\}$  in the dynamical core equations of motion  
432     and TE computations. Associated namelist changes resulting in this configuration are  
433     `lcp_moist = .false., se_qsize_condensate_loading = 1,` and `ftype = 1`.

434     The TE consistent configuration in AMIP-type simulation (*F2000climo*) is used to  
435     compute baseline TE tendencies which will be used to compare with other model con-  
436     figurations. First we establish how long an average is needed to get robust TE tendency  
437     estimates. Figure 2 shows  $\partial\hat{E}$  for various aspects of CAM-SE as a function of time. The  
438     simulation length is 5 years and monthly average values are used for the analysis. First  
439     consider the left plot. The TE tendency from parameterizations ( $\partial\hat{E}_{phys}^{(param)}$ ) show signif-  
440     icant variability with an amplitude of approximately  $2.5W/m^2$ . As noted above this term  
441     does not figure in the spurious TE budget. The net source/sink provides an equal and op-  
442     posite term to balance it. That said, the variability is reflected onto the TE tendency due  
443     to pressure work **error**  $\partial\hat{E}_{phys}^{(pwork)} \approx 0.32 \pm 0.08W/m^2$ . On the scale used in the left-  
444     hand plot the TE tendency of the adiabatic dynamical core  $\partial\hat{E}_{dyn}^{(adiab)}$  does not seem to be  
445     affected by  $\partial\hat{E}_{phys}^{(param)}$  or  $\partial\hat{E}_{phys}^{(pwork)}$  in terms of variability, and remains stable at approxi-  
446     mately  $-0.6W/m^2 \pm 0.02W/m^2$ . The TE fixer, in this model configuration, fixes  $\partial\hat{E}_{dyn}^{(adiab)}$   
447     and  $\partial\hat{E}_{phys}^{(pwork)}$ . Since the TE imbalance in the adiabatic dynamics remains approximately  
448     constant and the TE tendency associated with pressure work **error** has variability, the TE  
449     tendency from the  $\partial\hat{E}_{phys}^{(efix)}$  has variability;  $\partial\hat{E}_{phys}^{(efix)} \approx 0.30 \pm 0.08W/m^2$ . As a consistency  
450     check  $-\partial\hat{E}_{dyn}^{(adiab)} - \partial\hat{E}_{phys}^{(pwork)}$  is plotted with asterisk's and they coincide (as expected)  
451     with  $\partial\hat{E}_{phys}^{(efix)}$  fulfilling (22).

452     The right-hand plot in Figure 2 shows a breakdown of the dynamical core TE ten-  
453     dencies. The majority of the TE errors are due to hyperviscosity on temperature and pres-  
454     sure,  $\partial\hat{E}_{dyn}^{(hvis)} \approx -0.61 \pm 0.01W/m^2$ . The diffusion of momentum is added back as fric-  
455     tional heating and is therefore not part of  $\partial\hat{E}_{dyn}^{(hvis)}$ . The frictional heating is a significant  
456     term in the TE tendency budget  $\partial\hat{E}_{dyn}^{(fheat)} \approx 0.56 \pm 0.02W/m^2$  and exhibits some variabil-  
457     ity but with a rather small amplitude. The remaining TE error in the floating Lagrangian  
458     dynamics is inviscid dissipation and time-truncation errors  $\partial\hat{E}_{dyn}^{(res)} = \partial\hat{E}_{dyn}^{(2D)} - \partial\hat{E}_{dyn}^{(hvis)} \approx$   
459      $0.007W/m^2$ . The TE tendency from vertical remapping is approximately  $\partial\hat{E}_{dyn}^{(remap)} \approx$   
460      $-0.01W/m^2$ . To within  $\sim 0.02W/m^2$  the dynamical core TE tendency terms can be com-  
461     puted from just one month average TE integrals. The TE tendencies computed in physics,  
462     excluding  $\partial\hat{E}_{phys}^{(param)}$ , exhibit more variability and are only accurate to  $\sim 0.1W/m^2$  after a  
463     one month average.

464     While it is advantageous to use *state-update* physics-dynamics coupling algorithm  
465     (`ftype=1`) in terms of having no spurious TE tendency from coupling,  $\partial\hat{E}^{(pdc)} = 0$ ,  
466     it does result in spurious gravity waves in the simulations [see, e.g., Figure 5 in *Gross*  
467     *et al.*, 2018]. Figure 3a shows a 1 year average of  $|\frac{dp_s}{dt}|$ , a measure of high frequency  
468     gravity wave noise. It clearly exhibits unphysical oscillations coinciding with element  
469     boundaries. Details of the spectral-element method, its coupling to physics and associ-  
470     ated noise issues are discussed in detail in *Herrington et al.* [2018]. The noise in the solu-  
471     tions is even visible in the 500hPa pressure velocity annual average (Figure 4a). This  
472     issue can be alleviated by using a shorter physics time-step so that the physics increments  
473     are smaller (not shown). Climate modelers have historically not pursued a shorter physics  
474     time-step in production configurations as climate parameterizations are computationally

475 expensive and there is a large sensitivity to physics time-steps in the simulated climate  
 476 [e.g. Williamson and Olson, 2003; Wan *et al.*, 2015].

477 **3.2 ‘dribbling’ A/B: Non-TE conservative physics-dynamics coupling ( $f\text{type}=0, 2$ )**

478 **3.2.1 Element boundary noise**

479 When switching to *dribbling* physics-dynamics coupling algorithm ( $f\text{type}=0$ ) in  
 480 which the tendencies from physics are added throughout the dynamics (in this case twice  
 481 per physics time-step) then the noise issues described in previous section disappear (Figure  
 482 3b and 4b). That said, there is a significant issue with this approach; the tracer mass bud-  
 483 getes may not be closed. How this comes about is illustrated in Figure 5 and explained in  
 484 the next paragraph.

485 The orange curve on Figure 5a, b, d, and e is the initial state of, e.g., cloud liq-  
 486 uid mixing ratio as a function of location, e.g., longitude. Cloud liquid is zero outside  
 487 of clouds and hence provides a good example for the purpose of this illustration. The  
 488 light blue arrows show the increments (in terms of length of arrow) computed by the  
 489 parameterizations based on the initial state and scaled for the partial update with *dribbling*  
 490 ( $f\text{type}=0$ ). With *state-update* ( $f\text{type}=1$ ) the increments from physics are added to the  
 491 dynamical core state (dotted line on 5b) before the dynamical core advances the solution  
 492 in time. The parameterizations are designed to not drive the mixing ratios negative so the  
 493 state-update in dynamics will not generate negatives (or overshoots). Then the dynami-  
 494 cal core advects the distribution (solid curve on Figure 5c). With *dribbling* ( $f\text{type}=0$ ) the  
 495 physics increments are split into equal chunks (in this illustration two; blue errors on Fig-  
 496 ure 5d). Half of the physics increments are added to the initial state (dotted line on Fig-  
 497 ure 5e) and then dynamics advects the distribution half of the total dynamical core steps  
 498 (dashed line on Figure 5e). Then the other half of the physics increments are applied (in  
 499 the same location as they were computed by physics). Now after the previous/first advec-  
 500 tion step the cloud liquid distribution has moved and the mixing ratio may be zero (or  
 501 less than the increment prescribed by physics) where the physics forcing is applied (e.g.,  
 502 left side of dashed curve). Hence the physics increment is driving the mixing ratios neg-  
 503 ative in those locations. Thereafter the distribution is advected (solid curve on Figure 5f).  
 504 In CAM the increments added in the dynamical core are limited so that they drive the  
 505 mixing to zero (but not negative) if this problem occurs. This leads to a net source of  
 506 mass compared to the mass change that the parameterizations prescribe (see Figure 6).  
 507 Although the average source of mass is small each time-step it always has the same sign  
 508 (i.e. it is a bias) and therefore accumulates. Zhang *et al.* [2017] estimated that this spuri-  
 509 ous source of mass is equivalent to  $\sim 10\text{cm}$  sea-level rise per decade in coupled climate  
 510 simulation experiments.

511 The majority of the noise with *state-update* ( $f\text{type}=1$ ) physics-dynamics coupling  
 512 method comes from momentum sources/sinks and heating/cooling. A way to alleviate  
 513 noise problems and, at the same time, close the tracer mass budgets (in physics-dynamics  
 514 coupling) is to use *state-update* ( $f\text{type}=1$ ) coupling for tracers and *dribbling* ( $f\text{type}=0$ )  
 515 coupling for momentum and temperature (referred to as *combination*,  $f\text{type}=2$ ). Figure  
 516 3c shows the noise diagnostic  $|\frac{dp_s}{dt}|$  for *combination* ( $f\text{type}=2$ ) coupling. Figure 3c looks  
 517 very similar to Figure 3b but there is some noise near element boundaries. That said, in  
 518 terms of vertical pressure velocities *combination* ( $f\text{type}=2$ ) and *dribbling* ( $f\text{type}=0$ ) cli-  
 519 mates are similar in terms of the level of noise (Figure 4b and 4c). The element noise in  
 520 CAM-SE with *combination* ( $f\text{type}=2$ ) seen in both  $|\frac{dp_s}{dt}|$  and 500hPa pressure velocity  
 521 can be ‘removed’ by using CAM-SE-CSLAM (Figure 3d) which uses a quasi equal-area  
 522 physics grid and CSLAM [Conservative Semi-Lagrangian Multi-tracer; Lauritzen *et al.*,  
 523 2010] consistently coupled to the SE method [Lauritzen *et al.*, 2017]. The noise patterns  
 524 in vertical velocity off the western coast of South America are present in all CAM-SE

525 simulations (and hence not related to physics-dynamics coupling algorithm) are also ‘re-  
526 moved’ by using CAM-SE-CSLAM [Herrington *et al.*, 2018].

### 527 3.2.2 Spurious TE tendencies from physics-dynamics coupling

528 When using the same TE formula in the dynamical core and physics the spurious  
529 TE tendency from physics-dynamics coupling can be assessed. Since the pressure fields  
530 evolve during *dribbling* of physics forcing, the TE increments from the forcing change.  
531 For *dribbling* (`ftype=0`) and *combination* (`ftype=2`) this tendency is  $\partial\widehat{E}^{(pdc)} = -0.05W/m^2$   
532 and thus rather small compared to the viscosity TE dissipation rates. Since  $\partial\widehat{E}^{(pdc)}$  are  
533 the same (to the second digit) for *dribbling* (`ftype=0`) and *combination* (`ftype=2`) it is  
534 the momentum and temperature *dribbling* errors that dominate  $\partial\widehat{E}^{(pdc)}$ .

## 535 3.3 vert limiter: Limiters on vertical remapping of momentum

536 CAM-SE uses a floating Lagrangian vertical coordinate [Starr, 1945; Lin, 2004]  
537 which requires the remapping of the atmospheric state from floating levels back to refer-  
538 ence levels to maintain computational stability and to provide state data consistent with  
539 the physics formulation. The mapping algorithm is based on the mass conservative PPM  
540 (Piecewise Parabolic Method) with options for shape-preserving limiters. In CAM-SE mo-  
541 mentum components and internal energy are used as the variables mapped in the vertical  
542 [Lauritzen *et al.*, 2018] and, contrary to earlier versions of CAM-SE, there is no limiter  
543 on the remapping of wind components. If the shape-preserving limiter is used for mo-  
544 mentum mapping then the TE dissipation increases by over an order of magnitude from  
545  $\sim 0.01W/m^2$  to  $\sim 0.2W/m^2$  (Table 1).

## 546 3.4 smooth topo: Smoother topography

547 Topography for CAM is generated using a new version of the software/algorithm de-  
548 scribed in Lauritzen *et al.* [2015] that is available at <https://github.com/NCAR/Topo>.  
549 The updates to the software includes smoothing algorithms and the computation of sub-  
550 grid-scale orientation of topography.

551 The default topography in CAM-SE uses the same amount of topography smooth-  
552 ing as CAM-FV (distance weighted smoother applied to the raw topography on  $\sim 3\text{km}$   
553 cubed-sphere grid with a smoothing radius of 180km referred to as *C60*). When the to-  
554 graphy is smoother (in this case using *C92* smoothing, i.e. smoothing radius of approx-  
555 imately 276km) the hyperviscosity operators are less active leading to reduced TE errors,  
556 i.e.  $\partial\widehat{E}_{dyn}^{(hvvis)}$  is reduced in half from approximately  $-0.6W/m^2$  to  $-0.3W/m^2$ . The vertical  
557 remapping TE error, however, remains approximately the same. Since the pressure work  
558 **error** is approximately  $0.3W/m^2$  it almost exactly compensates for the TE tendency from  
559 the dynamical core  $\partial\widehat{E}_{dyn}^{(adiab)}$ . Hence if one would only diagnose the TE tendency from  
560 the energy fixer one could mistakenly conclude that the model universally conserves TE  
561 when, in fact, there are compensating TE errors in the system. These compensating errors  
562 can only be diagnosed through a careful breakdown of the total TE tendencies.

## 563 3.5 default: TE formula discrepancy errors

564 To assess the TE errors due to the discrepancy in the energy formula used by dy-  
565 namics and physics, a simulation using *state-updating* (`ftype=1`, no ‘*dribbling* errors’) and  
566 thermodynamically active condensates in the dynamical core (`qsize_condensate_loading =`  
567 5) and consistent/accurate associated heat capacities  $c_p^{(\ell)}$  (namelist `1cp_moist=.true.`)  
568 has been performed. In this setup the continuous equations of motion in the dynami-  
569 cal core conserve an energy different from physics, and the energy fixer will restore the  
570 ‘physics’ version of energy. Despite the dynamical core now using a more comprehensive  
571 formula for energy, the TE dissipation terms in the dynamical core are roughly the same

as in the energy consistent versions of the model. Using (25) we can assess the TE energy discrepancy errors which result in  $\sim 0.59W/m^2$ . *Taylor* [2011] found a similar result just from using the more comprehensive formula for heat capacity (based on dry air and water vapor) and not including thermodynamically active condensates. As noted before this formulation inconsistency is due to the evolutionary nature of CAM development and it is the intention to remove this inconsistency in future versions of the model.

The default version of CAM-SE uses this configuration but with *combination* (*ftype*=2) which has similar TE characteristics (see Table 1). That said, the physics-dynamics coupling error from *dribbling* momentum and temperature tendencies and the energy discrepancy errors can not be separated in this configuration:

$$\partial\widehat{E}^{(pdc)} + \partial\widehat{E}^{(discr)} = 0.546W/m^2, \quad (26)$$

using (22). With *state-updating* (*ftype*=1) (i.e.  $\partial\widehat{E}^{(pdc)} = 0$ ) the energy discrepancy error was  $0.594W/m^2$  and in the energy consistent setup (i.e.  $\partial\widehat{E}^{(discr)} = 0$ ) but using *dribbling* (*ftype*=2) we got  $\partial\widehat{E}^{(pdc)} = 0.484W/m^2$ . So if the physics-dynamics coupling errors and energy discrepancy errors in the different configurations would be additive, one would have expected  $\partial\widehat{E}^{(pdc)} + \partial\widehat{E}^{(discr)}$  to be over  $1W/m^2$  which is clearly not the case (26). Again, it must be concluded that there are canceling errors in the system.

### 3.6 QPC6: Simplified surface

By running the model in aqua-planet configuration one can assess the effect of simplifying the surface boundary condition. In particular, without topography forcing the dynamical core is not challenged with respect to stationary near-grid-scale forcing. The TE tendency with respect to pressure work *error* remains the same  $\partial\widehat{E}_{phys}^{(pwork)}$  as the AMIP-type simulations, however, the adiabatic dynamical core TE tendency reduces to  $\partial\widehat{E}_{dyn}^{(adiab)} = -0.14W/m^2$  (approximately a factor 4 reduction). Most of that reduction is due to viscosity  $\partial\widehat{E}_{dyn}^{(visc)} = -0.13W/m^2$ . The frictional heating is roughly the same as AMIP  $\partial\widehat{E}_{dyn}^{(fheat)} = 0.48W/m^2$  as is the vertical remapping  $\partial\widehat{E}_{dyn}^{(remap)} = -0.01W/m^2$ . To evaluate the dynamical cores diffusion of TE it is therefore important to asses the model in a configuration with topography as the wave dynamics generated by topography leads to more active diffusion operators.

### 3.7 FHS94: Simplified physics (no moisture)

Simplifying the setup even further by replacing the parameterizations with relaxation towards a zonally symmetric temperature profile and simple boundary layer friction (Held-Suarez forcing) as well as excluding moisture, the TE errors in the dynamical core decreases even further to  $\sim 0.002W/m^2$  since there is no small scale forcing. Small scales are only created by the nonlinear dynamics and the physics works to damp them. Hyper-viscosity is less active leading to significant reductions compared to aqua-planet and ‘real-world’ simulation results. The TE diffusion in vertical remapping reduces by an order of magnitude compared to the aqua-planet simulations ( $\sim 0.0005W/m^2$ ). This further emphasizes that TE diffusion assessment in a simplified setup is not necessarily telling for the dynamical cores performance with moist physics and topography that challenge the dynamical core in terms of strong grid-scale forcing.

### 3.8 FV: Changing dynamical core to Finite-Volume (FV)

As a comparison the TE error characteristics of the CAM-FV dynamical core are assessed. Although the TE diagnostics have not been implemented in the CAM-FV dynamical core, the TE diagnostics in CAM physics are independent of dynamical core and can therefore be activated with CAM-FV. The CAM-FV dynamical core uses *state-update* physics-dynamics coupling (*ftype*=1) ( $\partial\widehat{E}^{(pdc)} = 0$ ) and the same TE definition

as CAM physics ( $\partial\widehat{E}^{(discr)} = 0$ ). Hence (23) can be used to compute the TE errors of the CAM-FV dynamical core,  $\partial\widehat{E}_{dyn}^{(adiab)} \approx -1W/m^2$ . As we do not have the break-down of  $\partial\widehat{E}_{dyn}^{(adiab)}$  it can not be determined how much of the TE errors are due to the vertical remapping. Furthermore, CAM-FV contains intrinsic dissipation operators (limiters in the flux operators) making it difficult to assess TE sources/sinks due to dissipation. Note that the pressure work **error** even with a change of dynamical core remains approximately the same as the CAM-SE configurations.

### 3.9 CSLAM: Quasi equal-area physics grid

This configuration was discussed in the context of element noise in section 3.2.1. By averaging the dynamics state of an equal-partitioning (in central angle cubed-sphere coordinates) of the elements, the element-boundary noise found in CAM-SE can be removed. Lauritzen *et al.* [2018] argue that this way of computing the state for the physics is more consistent with physics in terms of providing a cell-averaged state instead of irregularly spaced point (quadrature) values. In order to achieve a closed mass-budget, this configuration uses CSLAM for tracer transport rather than SE transport. That said, the physics columns no longer coincide with the quadrature grid and there are TE errors associated with mapping state and tendencies between the two grids.

In this configuration the energy diagnostics computed in the dynamical core are computed on the quadrature grid and the energy diagnostics computed in physics are on the physics grid. If the TE consistent configuration is used (`ftype=1, qsize_condensate_loading=1, lcp_moist=.false.`) then the physics-dynamical coupling errors,  $\widehat{E}^{(pdc)}$  computed with (20), are entirely due to mapping state from quadrature grid to physics grid and mapping tendencies back the quadrature grid from the physics grid. The results is  $\widehat{E}^{(pdc)} = -0.07W/m^2$  which is a rather small error compared to other terms in the TE budget.

Due to similar noise problems with CAM-SE-CSLAM when using `ftype=1` that were observed in CAM-SE (Figure 3 and 4), the default version of CAM-SE-CSLAM uses `ftype=2`. Again physics-dynamics coupling errors and TE discrepancy errors can not be separated;  $\partial\widehat{E}^{(pdc)} + \partial\widehat{E}^{(discr)} = 0.557W/m^2$ .

## 4 Conclusions

A detailed total energy (TE) error analysis of the Community Atmosphere Model (CAM) using version 6 physics (included in the CESM2.1 release) running at approximately  $1^\circ$  horizontal resolution has been presented. In the global climate model there can be many spurious contributions to the TE budget. These errors can be divided into four categories: physical parameterizations, adiabatic dynamical core, the coupling between physics and dynamics, and TE definition discrepancies between dynamics and physics. The latter is not by design but through the evolutionary nature of model development. By capturing the atmospheric state at various locations in the model algorithm, a detailed budget of TE errors can be constructed. The net spurious TE energy errors are compensated with a global energy fixer (providing a global uniform temperature increment) every physics time-step.

In CAM physics the parameterizations have, by design, a closed energy budget (change in TE is balanced by fluxes in/out the top and bottom of physics columns) if it is assumed that pressure is not modified. However, the pressure changes due to fluxes of mass (e.g., water vapor) in/out of the column which changes energy (referred to as pressure work **error**). The pressure work **error** with the full moist physics configuration is very stable across different configurations at  $\sim 0.3W/m^2$ . The TE errors in the spectral element (SE) dynamical core varies across configurations. Aspects that influence TE is the presence of topography, the amount of topography smoothing and moist physics. By smoothing topography more the TE error is cut in half from  $\sim -0.6W/m^2$  to  $\sim -0.3W/m^2$ ; and re-

duces by a factor of **six** ( $\sim -0.1W/m^2$ ) if no topography is present at all (aqua-planet configuration). Moist physics forcing also contributes significantly to the TE budget. For example, in the dry Held-Suarez setup TE dissipation of the SE dynamical core reduces to  $-0.03W/m^2$ . Topography and moist physics force the dynamical core at the grid scale and hence the viscosity operators are more active. Consistent with this statement is that the changes in TE discussed so far are almost entirely due to the viscosity operator TE dissipation. For CAM-SE the spurious TE dissipation in the adiabatic dynamical core is  $\sim -0.6W/m^2$  in ‘real-world’ configurations. For comparison, CAM-FV’s spurious TE change due to the adiabatic dynamical core is  $\sim -1W/m^2$ .

By further breaking down the TE dissipation in the SE dynamical core it is observed the vertical remapping accounts for only  $\sim -0.01W/m^2$ . That said, if the shape-preserving limiters in the vertical remapping are invoked the TE dissipation increases 20-fold to  $\sim -0.2W/m^2$ . In CAM-SE the kinetic energy dissipation is added as heating in the thermodynamic equation (also referred to as frictional heating). The frictional heating remains very stable across configurations that include moisture ( $\sim 0.5W/m^2$ ) and reduces drastically for dry atmosphere setups (factor 4 reduction to  $(\sim 0.12W/m^2)$ ). Hence this term is an important term in the TE budget. The TE budget for the dynamical core is dominated by TE change due to hyperviscosity; TE errors due to time-truncation and frictionless equations of motion are negligible. Errors associated with physics-dynamics coupling (if applicable) are approximately  $0.5W/m^2$ . Due to the evolutionary nature of model development the SE dynamical core’s continuous equation of motion conserve a more comprehensive TE compared to the physical parameterizations. This TE discrepancy leads to an approximately  $0.5W/m^2$  total energy source. Running physics on a different grid than the dynamical introduces TE mapping errors such as in CAM-SE-CSLAM (Conservative Semi-Lagrangian Multi-tracer transport scheme). These errors are, however, rather small  $-0.07W/m^2$ .

A purpose of this paper is to better understand the energy characteristics of CAM and to encourage modeling groups to perform similar analysis to better understand the total energy flow in the atmospheric component of Earth system models. As has been demonstrated in this paper there can easily be compensating errors in the system which can not be identified without a detailed TE analysis.

## Acknowledgments

The National Center for Atmospheric Research is sponsored by the National Science Foundation. Computing resources (doi:10.5065/D6RX99HX) were provided by the Climate Simulation Laboratory at NCAR’s Computational and Information Systems Laboratory, sponsored by the National Science Foundation and other agencies. The data used to perform the energy analysis can be found at <https://github.com/PeterHjortLauritzen/2018-JAMES-energy>.

## References

- Boville, B. (2000), chap. Toward a complete model of the climate system in Numerical Modeling of the Global Atmosphere in the Climate System, pp. 419–442, Springer Netherlands.
- Computational and Information Systems Laboratory (2017), Cheyenne: HPE/SGI ICE XA System (Climate Simulation Laboratory), Boulder, CO: National Center for Atmospheric Research, doi:10.5065/D6RX99HX.
- Eldred, C., and D. Randall (2017), Total energy and potential enstrophy conserving schemes for the shallow water equations using hamiltonian methods – part 1: Derivation and properties, *Geosci. Model Dev.*, 10(2), 791–810, doi:10.5194/gmd-10-791-2017.

- Gross, M., H. Wan, P. J. Rasch, P. M. Caldwell, D. L. Williamson, D. Klocke, C. Jablonowski, D. R. Thatcher, N. Wood, M. Cullen, B. Beare, M. Willett, F. Lemarié, E. Blayo, S. Malardel, P. Termonia, A. Gassmann, P. H. Lauritzen, H. Johansen, C. M. Zarzycki, K. Sakaguchi, and R. Leung (2018), Physics-dynamics coupling in weather, climate and earth system models: Challenges and recent progress, *Mon. Wea. Rev.*, 146, 3505–3544, doi:10.1175/MWR-D-17-0345.1.
- Held, I. M., and M. J. Suarez (1994), A proposal for the intercomparison of the dynamical cores of atmospheric general circulation models, *Bull. Amer. Meteor. Soc.*, 75, 1825–1830.
- Herrington, A. R., P. H. Lauritzen, M. A. Taylor, S. Goldhaber, B. E. Eaton, K. A. Reed, and P. A. Ullrich (2018), Physics-dynamics coupling with element-based high-order Galerkin methods: quasi equal-area physics grid, *Mon. Wea. Rev.*
- Jablonowski, C., and D. L. Williamson (2011), chap. The Pros and Cons of Diffusion, Filters and Fixers in Atmospheric General Circulation Models, pp. 381–493, Springer Berlin Heidelberg, Berlin, Heidelberg, doi:10.1007/978-3-642-11640-7\_13.
- Kasahara, A. (1974), Various vertical coordinate systems used for numerical weather prediction, *Mon. Wea. Rev.*, 102(7), 509–522.
- Lauritzen, P. H., R. D. Nair, and P. A. Ullrich (2010), A conservative semi-Lagrangian multi-tracer transport scheme (CSLAM) on the cubed-sphere grid, *J. Comput. Phys.*, 229, 1401–1424, doi:10.1016/j.jcp.2009.10.036.
- Lauritzen, P. H., J. T. Bacmeister, T. Dubos, S. Lebonnois, and M. A. Taylor (2014), Held-Suarez simulations with the Community Atmosphere Model Spectral Element (CAM-SE) dynamical core: A global axial angular momentum analysis using Eulerian and floating Lagrangian vertical coordinates, *J. Adv. Model. Earth Syst.*, 6, doi: 10.1002/2013MS000268.
- Lauritzen, P. H., J. T. Bacmeister, P. F. Callaghan, and M. A. Taylor (2015), NCAR\_Topo (v1.0): NCAR global model topography generation software for unstructured grids, *Geosci. Model Dev.*, 8(12), 3975–3986, doi:10.5194/gmd-8-3975-2015.
- Lauritzen, P. H., M. A. Taylor, J. Overfelt, P. A. Ullrich, R. D. Nair, S. Goldhaber, and R. Kelly (2017), CAM-SE-CSLAM: Consistent coupling of a conservative semi-lagrangian finite-volume method with spectral element dynamics, *Mon. Wea. Rev.*, 145(3), 833–855, doi:10.1175/MWR-D-16-0258.1.
- Lauritzen, P. H., R. Nair, A. Herrington, P. Callaghan, S. Goldhaber, J. Dennis, J. T. Bacmeister, B. Eaton, C. Zarzycki, M. A. Taylor, A. Gettelman, R. Neale, B. Dobbins, K. Reed, and T. Dubos (2018), NCAR release of CAM-SE in CESM2.0: A reformulation of the spectral-element dynamical core in dry-mass vertical coordinates with comprehensive treatment of condensates and energy, *J. Adv. Model. Earth Syst.*, doi: 10.1029/2017MS001257.
- Lin, S.-J. (2004), A 'vertically Lagrangian' finite-volume dynamical core for global models, *Mon. Wea. Rev.*, 132, 2293–2307.
- McRae, A. T. T., and C. J. Cotter (2013), Energy- and enstrophy-conserving schemes for the shallow-water equations, based on mimetic finite elements, *Quart. J. Roy. Meteor. Soc.*, 140(684), 2223–2234, doi:10.1002/qj.2291.
- Medeiros, B., D. L. Williamson, and J. G. Olson (2016), Reference aquaplanet climate in the community atmosphere model, version 5, *J. Adv. Model. Earth Syst.*, 8(1), 406–424, doi:10.1002/2015MS000593.
- Neale, R. B., and B. J. Hoskins (2000), A standard test for AGCMs including their physical parametrizations: I: the proposal, *Atmos. Sci. Lett.*, 1(2), 101–107, doi:10.1006/asle.2000.0022.
- Neale, R. B., C.-C. Chen, A. Gettelman, P. H. Lauritzen, S. Park, D. L. Williamson, A. J. Conley, R. Garcia, D. Kinnison, J.-F. Lamarque, D. Marsh, M. Mills, A. K. Smith, S. Tilmes, F. Vitt, P. Cameron-Smith, W. D. Collins, M. J. Iacono, R. C. Easter, S. J. Ghan, X. Liu, P. J. Rasch, and M. A. Taylor (2012), Description of the NCAR Community Atmosphere Model (CAM 5.0), *NCAR Technical Note NCAR/TN-486+STR*, National

- 772 Center of Atmospheric Research.
- 773 Skamarock, W. C., J. B. Klemp, M. G. Duda, L. Fowler, S.-H. Park, and T. D. Ringler  
 774 (2012), A multi-scale nonhydrostatic atmospheric model using centroidal Voronoi tes-  
 775 selations and C-grid staggering, *Mon. Wea. Rev.*, 140, 3090–3105, doi:doi:10.1175/  
 776 MWR-D-11-00215.1.
- 777 Starr, V. P. (1945), A quasi-Lagrangian system of hydrodynamical equations., *J. Atmos.*  
 778 *Sci.*, 2, 227–237.
- 779 Taylor, M. A. (2011), Conservation of mass and energy for the moist atmospheric prim-  
 780 itive equations on unstructured grids, in: P.H. Lauritzen, R.D. Nair, C. Jablonowski,  
 781 M. Taylor (Eds.), Numerical techniques for global atmospheric models, *Lecture Notes*  
 782 in Computational Science and Engineering, Springer, 2010, *in press.*, 80, 357–380, doi:  
 783 10.1007/978-3-642-11640-7\_12.
- 784 Thuburn, J. (2008), Some conservation issues for the dynamical cores of NWP and cli-  
 785 mate models, *J. Comput. Phys.*, 227, 3715–3730.
- 786 Trenberth, K. E., and J. T. Fasullo (2018), Applications of an updated atmospheric ener-  
 787 getics formulation, *J. Climate*, 31(16), 6263–6279, doi:10.1175/JCLI-D-17-0838.1.
- 788 Wan, H., P. J. Rasch, M. A. Taylor, and C. Jablonowski (2015), Short-term time step con-  
 789 vergence in a climate model, *J. Adv. Model. Earth Syst.*, 7(1), 215–225, doi:10.1002/  
 790 2014MS000368.
- 791 Williamson, D. L. (2002), Time-split versus process-split coupling of parameterizations  
 792 and dynamical core, *Mon. Wea. Rev.*, 130, 2024–2041.
- 793 Williamson, D. L., and J. G. Olson (2003), Dependence of aqua-planet simulations on  
 794 time step, *Q. J. R. Meteorol. Soc.*, 129(591), 2049–2064.
- 795 Williamson, D. L., J. G. Olson, C. Hannay, T. Tonizzo, M. Taylor, and V. Yudin (2015),  
 796 Energy considerations in the community atmosphere model (cam), *J. Adv. Model. Earth*  
 797 *Syst.*, 7(3), 1178–1188, doi:10.1002/2015MS000448.
- 798 Zhang, K., P. J. Rasch, M. A. Taylor, H. Wan, L.-Y. R. Leung, P.-L. Ma, J.-C. Golaz,  
 799 J. Wolfe, W. Lin, B. Singh, S. Burrows, J.-H. Yoon, H. Wang, Y. Qian, Q. Tang,  
 800 P. Caldwell, and S. Xie (2017), Impact of numerical choices on water conservation in  
 801 the e3sm atmosphere model version 1 (eam v1), *Geoscientific Model Development Dis-  
 802 cussions*, 2017, 1–26, doi:10.5194/gmd-2017-293.

```

do nt=1,ntotal

PARAMETERIZATIONS:
Last dynamics state received from dynamics
output 'pBF'
efix Energy fixer
output 'pBP'
phys param Physics updates the state and state saved for energy fixer
output 'pAP'
pwork Pressure work (dry mass correction)
output 'pAM'
Physics tendency (forcing) passed to dynamics

DYNAMICAL CORE
output 'dED'
do ns=1,nsplit
output 'dAF'

phys
START PHYSICS-DYNAMICS COUPLING
Update dynamics state with (1/nsplit) of physics tendency (ftype=2)
if (ns=1) Update dynamics state with entire physics tendency (ftype=1)
DONE PHYSICS-DYNAMICS COUPLING

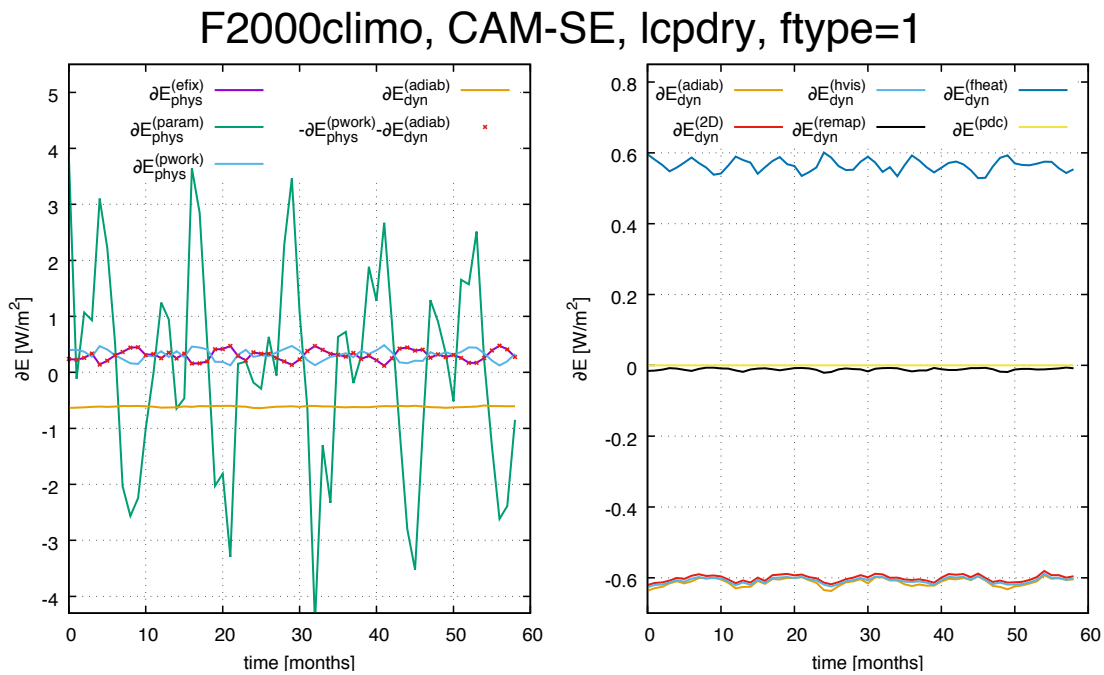
output 'dB'D'

adiab
2D
hvis
do nr=1,rsplit
Advance the adiabatic frictionless equations of motion
in floating Lagrangian layer
do ns=1,hypervis_subcycle
output 'dBH'
Apply hyperviscosity operators
output 'dCH'
fheat Add frictional heating to temperature
output 'dAH'
end do (ns=1,hypervis_subcycle)
end do (nr=1,rsplit)
output 'dAD'
remap
Vertical remapping from floating Lagrangian levels to Eulerian levels
output 'dAR'
end do (ns=1,nsplit)
Dynamics state saved for next model time step and passed to physics
output 'dB'F'

end do (nt=1,ntotal)

```

270 **Figure 1.** Pseudo-code for CAM-SE showing the order in which relevant physics updates are performed as  
271 well as dynamical core steps and associated loops. In green font locations where the state is captured and out-  
272 put is shown together with its 3 character identifier. The outer most loop (1, *ntotal*) advances the entire model  
273  $\Delta t_{phys}$  seconds (in this case 1800s). The dynamical core loops are as follows: the outer loop is the vertical  
274 remapping loop (1, *nsplit*) with associated time-step  $\Delta t_{phys}/nsplit$ . For stability the temporal advance-  
275 ment of the equations of motion in the Lagrangian layer needs to be sub-cycled *rsplit* times. Within the  
276 *rsplit*-loop the hyperviscosity time-stepping is sub-cycled *hypervis\_subcycle* times (again for stability).  
277 For more details on the time-stepping in CAM-SE see Lauritzen *et al.* [2018].



419 **Figure 2.** Monthly averaged TE tendencies as a function of time for various aspects of the TE consistent  
 420 configuration of CAM-SE run in AMIP-type configuration with perpetual year 2000 SSTs. Left Figure shows  
 421  $\partial \hat{E}$  TE tendencies in physics and, for comparison, TE tendency for the adiabatic dynamical core. The right  
 422 plot shows the break-down of  $\partial \hat{E}$  for the dynamical core. These plots show that the energy tendency from the  
 423 dynamical core is quite constant (to within  $\sim 0.02 W/m^2$  or less) so only one month simulations is adequate to  
 424 assess energy diagnostics for the dynamical core. For more details see Section 3.1.

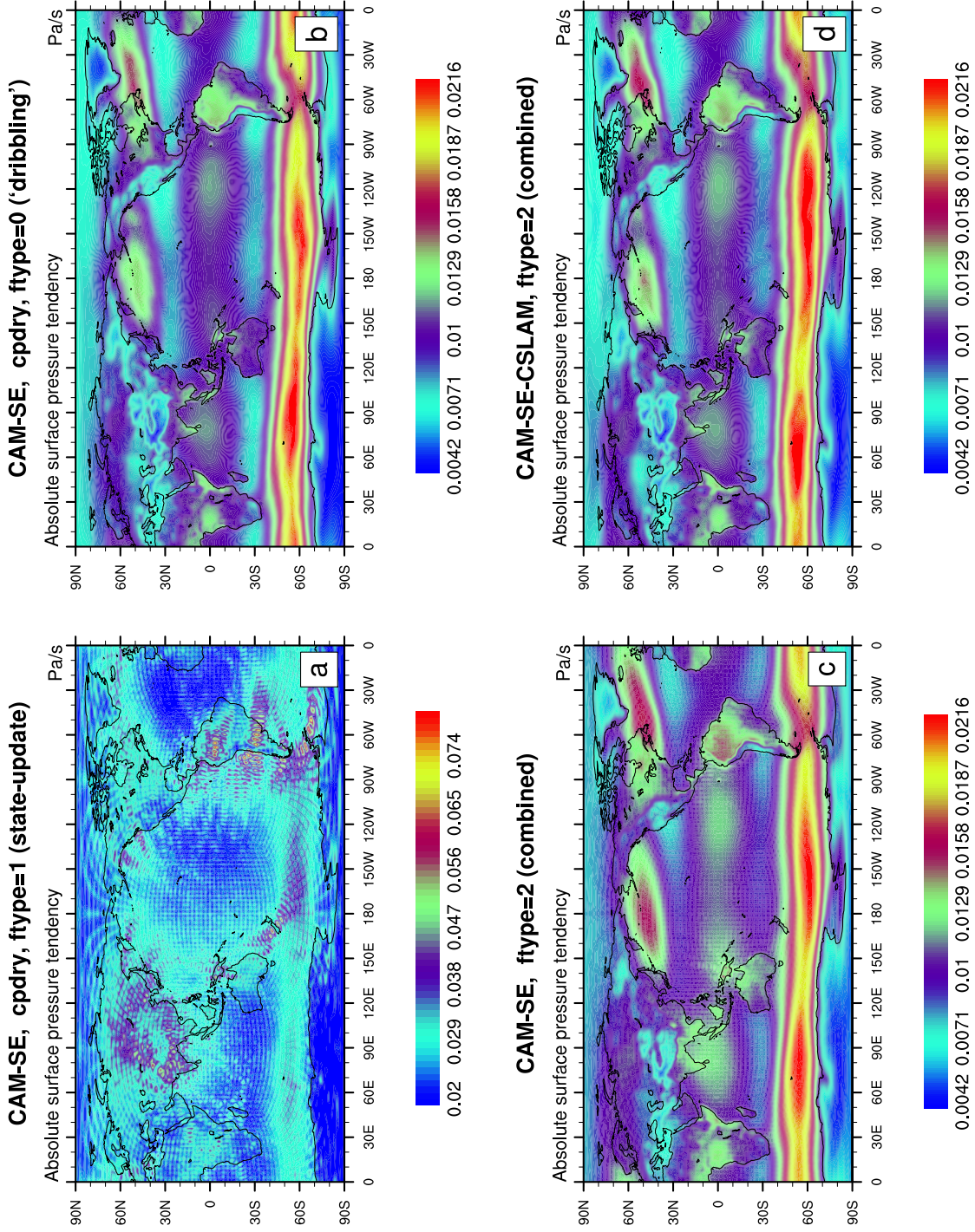


**Figure 3.** One year average of the absolute surface pressure tendency for (a) the TE consistent configuration, (b) ‘dribbling’ physics-dynamics coupling, (c) ftype=2 physics-dynamics coupling and (d) CSLAM version of CAM-SE, respectively. (a) has a closed physics-dynamics coupling budget but spurious noise, (b) has no spurious noise but the mass-budget in physics-dynamics coupling is not closed (see Figure 6), (c) has a closed mass budget in physics-dynamics coupling but some spurious noise at element boundaries which is eliminated when using CAM-SE-CSLAM (d). Note, the smallest value in panel (a) is the largest in panels (b), (c) and (d).

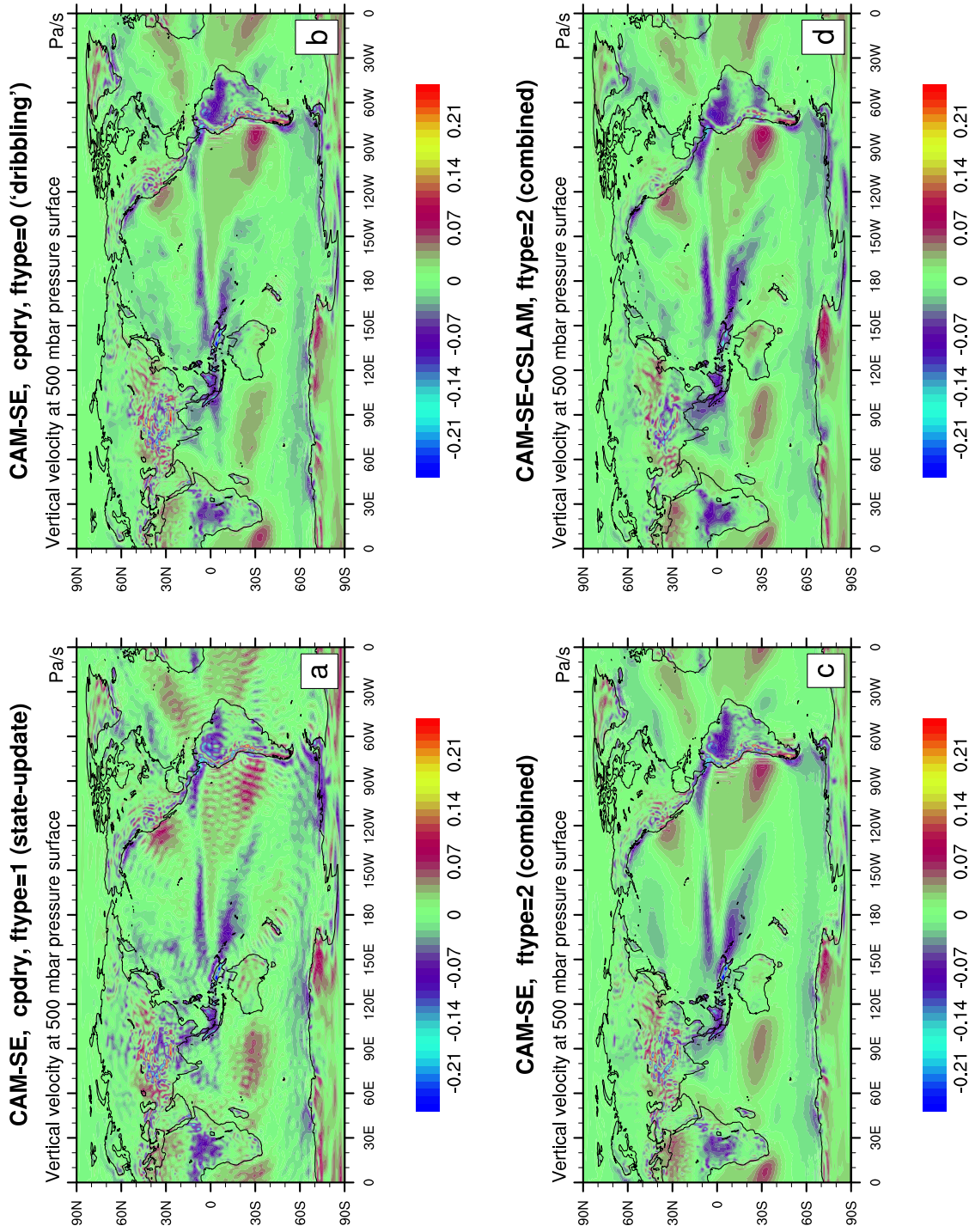


**Figure 4.** Same as Figure 3 but for 500hPa vertical pressure velocity. Note the ringing patterns off the West coast of South America and around the Himalayas in CAM-SE (a-c) that are eliminated with CAM-SE-CSLAM (d) that makes use of a quasi equal-area physics grid.

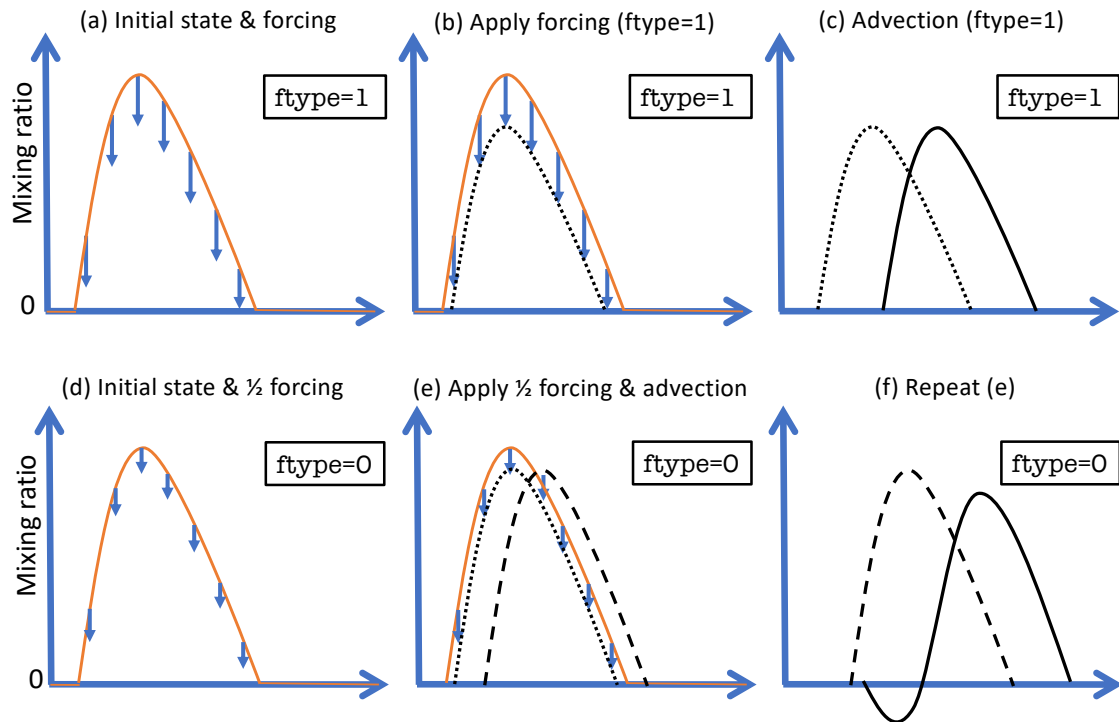


**Figure 5.** A schematic of state-update ( $\text{ftype}=1$ ; row 1) and ‘dribbling’ ( $\text{ftype}=0$ ; row 2) physics-dynamics coupling algorithms. See Section 3.2 for details.

## F2000climo, CAM-SE, cpdry, ftype=0 ('dribbling')

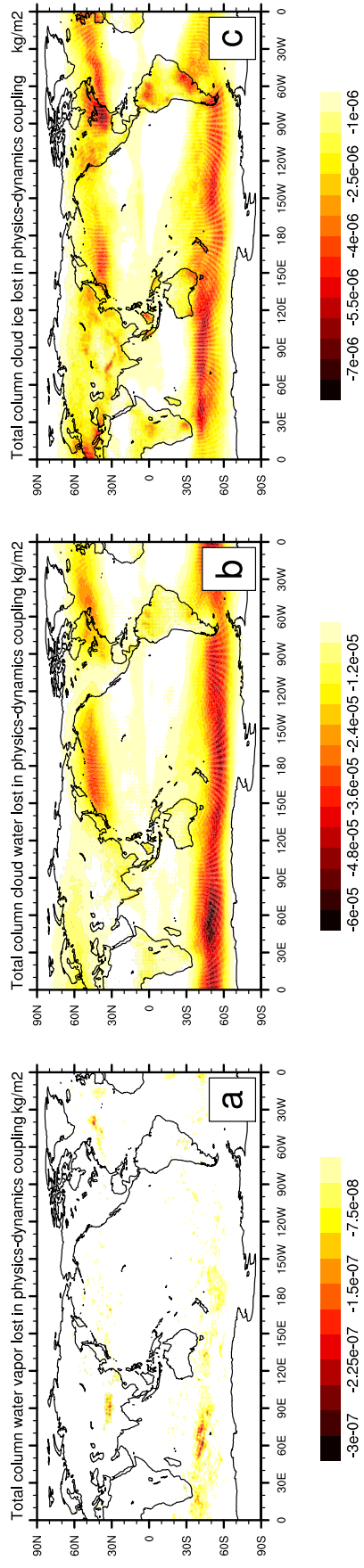


**Figure 6.** One year average of mass [ $\text{kg}/\text{m}^2$ ] 'clipped' in physics-dynamics coupling (so that state is not driven negative) when using `ftype=0` ('dribbling') physics-dynamics coupling for (a) water vapor, (b) cloud liquid and (c) cloud ice, respectively. Interestingly the element boundaries systematically show in the plots which is likely related to the anisotropy of the quadrature grid [Herrington *et al.*, 2018].